

Delay Profile Measurement System for Microwave Mobile Communications and Delay Characteristics in an Urban Environment

Takehiko Kobayashi, Hironari Masui, Satoshi Takahashi, Koichi Takahashi, and Kouzou Kage

YRP Key Tech Labs

3-4 Hikarino-oka, Yokosuka, 239-0847 Japan

Phone: +81 468 47 5303 Fax.: +81 468 47 5305 E-mail: koba@yrp-ktrl.co.jp

Abstract— We have developed a system for measuring the microwave broadband propagation delay profile over 100-MHz spread bandwidths in the 3, 8, and 16 GHz bands. Experiments confirmed the system has a time resolution of 20 ns, maximum measurable delay of 40 μ s, relative amplitude error of within 3 dB and dynamic range of over 60 dB. We used the system to measure line-of-sight delay profiles in an urban area and particularly studied effects of mobile antenna height. We found that delay spreads increase with increasing transmit/receive distance and become larger at the lower antenna height.

I. INTRODUCTION

The exploitation of new frequency bands has recently become a very important theme because of the dramatic growth in the demand for mobile radio communications. Furthermore, the development of multimedia mobile communication systems with voice, image, and mass-data transmission capabilities is advancing rapidly, so efficient spectrum utilization is necessary. The microwave band is considered a candidate for the broadband mobile communications; and microcellular systems are expected to use frequencies above the microwave band [1]-[3]. However, the propagation characteristics of mobile communications in the microwave band have not yet been sufficiently studied.

Understanding propagation delay is essential to studying propagation mechanisms and designing Rake receivers. Several methods for measuring delay profile [4] have been developed. Of these, we chose a method utilizing a pseudo noise (PN) code [5] because of its high precision in outdoor experiments. Our system works with microwave frequencies in the 3 to 16 GHz range and a bandwidth of 100 MHz.

The developed system was used to measure and analyze delay profiles in an urban area with line of sight, and we focused on mobile antenna height (h_M). The delay spreads at different transmitter and receiver distances [6] were measured at $h_M = 1.6$ and 2.7 m.

II. SYSTEM DESCRIPTION

The system must satisfy the following

performance requirements:

- High resolution (20 ns) at high transmission rate (50 Mchip/s).
- Wide dynamic range (60 dB) and long measurable delay time (40 μ s) at long code length (2047 chips).
- If the maximum Doppler shift is 1 kHz, the minimum measurement interval should be 50 μ s; accordingly, a time constant of automatic gain control (AGC) in the receiver should be short enough to meet this objective .

A. Transmitter

The transmitter (Fig. 1) of this system is capable of transmitting microwaves at a center frequency (f_c) of 3.35, 8.45, or 15.75 GHz modulated by a PN code with a transmission rate of 50 Mchip/s. A rubidium (Rb) oscillator is used as the master clock, which provides frequency stability within 3×10^{-12} , to stabilize the carrier frequency and maintain the synchronization of the transmitter and receiver. The rate needed to achieve long-term stability is given by [resolution] / [measurement time period][7]. It is 5.6×10^{-12} at a resolution of 20 ns and a measurement time period of 1 hour. A Rb oscillator is thus capable of maintaining sufficient stability.

The transmitter has a waveform memory and a high-speed (400 Msample/s) digital-to-analog converter to generate the 50-Mchip/s baseband signal of PN code of M sequence from 7 to 11 stages. This baseband signal is modulated to 3.35 GHz by a binary phase shift keying (BPSK) modulator and then further frequency-converted to 8.45 and 15.75 GHz. Next, the signal is amplified to 10 W by using a power amplifier with an automatic level control

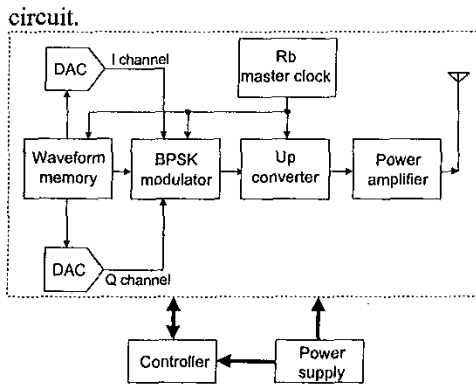


Fig. 1. Transmitter block diagram.

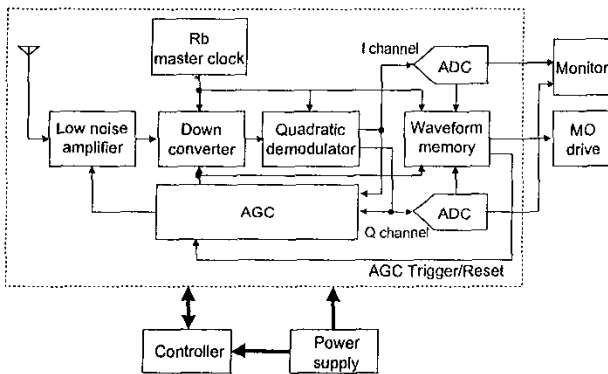


Fig. 2. Receiver block diagram.

B. Receiver

A single super-heterodyne configuration is used as shown in Fig. 2. The radiofrequency signal is first converted to the intermediate frequency of 5.1 GHz, then orthogonal detection is used to extract the in-phase (I) and quadrature (Q) components. A R_b oscillator, like the one used in the transmitter unit, is used as the master clock for the local oscillator and for the analog-to-digital (A/D) converter's sample timing. The I and Q components are quantized by 10-bit A/D conversion and stored directly in a 1-Gbyte waveform memory. With double oversampling, the sampling rate of this measuring system is 100 Msample/s.

Fading causes high momentary fluctuations of over 20 dB at the received level. In addition, the received signal suffers short- and long-term median variations. In response to these wide fluctuations and

variations, an AGC circuit (Fig. 3) is incorporated in the receiver to effectively utilize the resolution of 10-

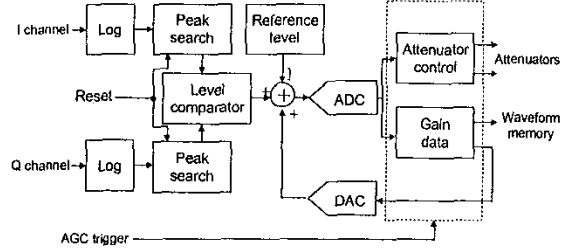


Fig. 3. AGC block diagram.

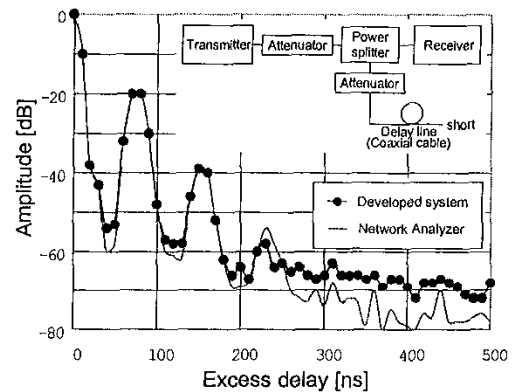


Fig. 4. Comparison with network analyzer measurement (code length = 2047).

bit A/D conversion. To ensure high-speed and reliable AGC operation, we extracted the peak value of the I or Q component, whichever was larger, and used a lookup table to set the system gain according to this value. As a result, the AGC time constant was 2 μ s in a 50-dB dynamic range in 1-dB steps. Correlation between the transmitted PN code and the received signal (I and Q components) is carried out off-line to compute the delay profiles, which are compensated by the AGC data. Up to 32 continuous delay profiles are used to provide ensemble averages.

A monitor in the receiver enables us to on-site check the data obtained through measurements. The monitor was used to observe an outline of the delay profile in quasi-real time. The observation involved using a digital signal processor to perform product-sum operations on a portion of the quantized output. The lookup table was also used to enable

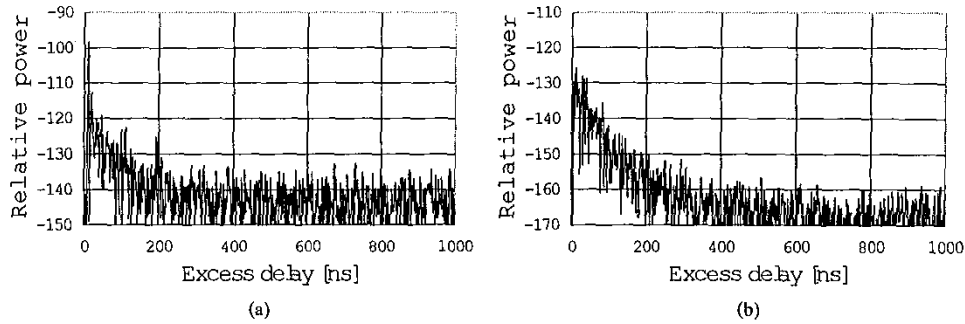


Fig. 5. Examples of measured delay profiles ($d = 800$ m, $h_B = 4$ m, $f_c = 3.35$ GHz). (a) $h_M = 2.7$ m. (b) $h_M = 1.6$ m.

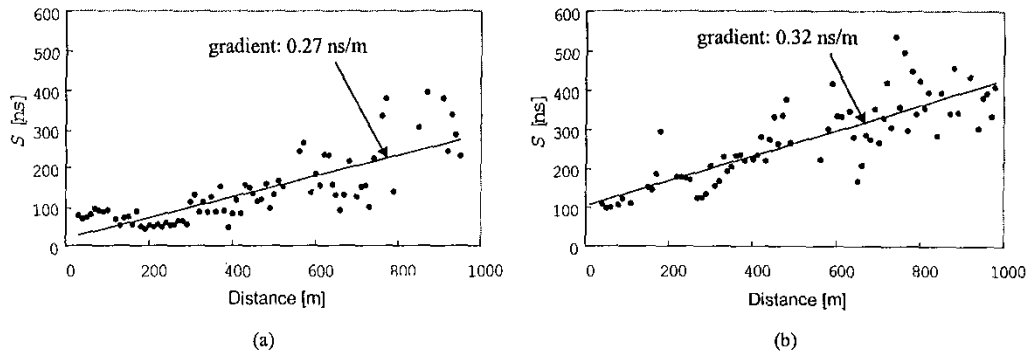


Fig. 6. Distance dependence of delay spreads ($d = 800$ m, $h_B = 4$ m, $f_c = 3.35$ GHz). (a) $h_M = 2.7$ m. (b) $h_M = 1.6$ m.

simultaneous display of the envelope in dB.

C. Evaluating System Performance

To evaluate the system performance, we compared the delay profiles independently measured with this system in the time domain and with a microwave network analyzer in the frequency domain. Stable delay waves were generated by using a microwave power splitter, two attenuators, and coaxial cable with the end shorted.

The measured performance of the system and that of the network analyzer almost agree, as shown in Fig. 4. The difference between these measurements is within 3 dB. The dynamic range of the system is evaluated to be more than 60 dB; that is, close to the theoretical value of 66 dB ($= 20 \log 2047$) for an 11-step PN coding length. Designed time resolution of 20 ns at -3 -dB peak width was also obtained.

III. MEASUREMENT AND ANALYSIS OF DELAY

CHARACTERISTICS

The developed system was used to measure the line-of-sight delay profiles in a metropolitan Tokyo area. Measurements were made under daytime traffic conditions along a 1-km stretch of straight road (width of 27 m) near Tokyo station. Focusing on mobile antenna height (h_M), we compared measured delay when the receiver antenna was positioned on a handcart ($h_M = 1.6$ m) and when it was positioned on the roof of a vehicle ($h_M = 2.7$ m). And the base-station antenna height h_B was 1.6 m. Vertical half-wavelength dipole antennas were used for both transmission and reception. The continuous 32 data with a spread length of 2047 chips were recorded at every 2 m along the measurement course. The average delay profile was calculated from these data and used for calculating delay spreads.

Typical examples of delay profiles are shown in Fig. 5. Different mobile antenna heights at each point produced different delay profiles. When $h_M = 1.6$ m, the drop in the relative power with increasing

excess delay is more severe than that when $h_M = 2.7$ m.

Taking into account the arriving waves within 30 dB of the peak of the first arriving wave, the delay spreads (S) were calculated from these delay profiles. The delay spreads, averaged for every 10m along the measurement course, are plotted against the transmit/receive distance (d) in Fig. 6. At either h_M , the delay spread and its variance increase with increasing distance. Delay spreads at $h_M = 1.6$ m are larger than those at $h_M = 2.7$ m at almost all measurement locations. Linear approximation resulted in a gradient of 0.27 ns/m at $h_M = 2.7$ m and 0.32 ns/m at $h_M = 1.6$ m. From these results, we infer that, in the portable mode ($h_M = 1.6$ m), the line of sight is deteriorated by the shadowing effect of the pedestrians and vehicles on the road, because antenna height is about the same as the average equivalent road height [8], [9]. Typically, the difference between the peak powers of the first and second arriving waves was larger than 10 dB at $h_M = 2.7$ m, but only a few dB at $h_M = 1.6$ m. This difference also suggests that the more frequent blocking of line of sight at lower h_M results in longer delay spreads.

IV. Summary

We have developed a system capable of measuring delay profiles of microwaves at 3.35, 8.45, and 15.75 GHz frequencies and a transmission rate of 50 Mchip/s (equivalent to time resolution of 20 ns or distance resolution of 6 m).

This system was used to measure the delay characteristics in the microwave band on a line-of-sight street located in an urban area. It was found that the measured delay spread and its variance increase with increasing distance (d) between the transmitter and receiver, and the delay spreads and their gradients against d are greater at $h_M = 1.6$ m than those at $h_M = 2.7$ m.

ACKNOWLEDGMENT

The authors would like to extend their appreciation to Dr. K. Taira of the Communication Research Laboratories for his helpful advice throughout the development of this system. They also like to thank the engineers at Advantest Corporation for constructing the system.

REFERENCES

- [1] K. Taira, S. Sekizawa, G. Wu, H. Harada, and Y. Hase, "Propagation loss characteristics for microcellular mobile communications in microwave band," in *IEEE Int. Conf. Universal Personal Commun.*, Cambridge, MA, Sept.-Oct. 1996, pp. 842-846.
- [2] Y. Oda, T. Tanaka, and K. Satoh, "Microwave band LOS path loss characteristics in microcellular mobile communications," in *Proc. Int. Symp. Antennas. Propag.*, Makuhari, Japan, Sept. 1996, pp. 1097-1100.
- [3] G. Durgin, T. S. Rappaport, and H. Xu, "Radio path loss and penetration loss measurements in and around homes and trees at 5.85 GHz," in *IEEE Antennas Propagat. Soc. Int. Symp.*, Atlanta, GA, June 1998, pp. 618-621.
- [4] K. Pahlavan and A. H. Levesque, *Wireless Information Networks*. New York: John Wiley & Sons, 1995, Chap. 5.
- [5] D. C. Cox, "Delay doppler characteristics of multipath propagation at 910 MHz in a suburban mobile radio environment," *IEEE Trans. Antennas. Propagat.*, vol. 20, no. 5, pp. 625-635, May 1972.
- [6] S. Ichitsubo, T. Furuno, and R. Kawasaki, "A delay profile model for microcell multipath propagation in urban areasV" *IEICE Trans. B-II*, vol. J80-B-II, no. 8, pp.707-713, Aug. 1997 (in Japanese).
- [7] D. Parsons, *The Mobile Radio Propagation Channel*. London, U.K.: Pentech Press, 1992, pp. 231-232.
- [8] Y. Oda and K. Tsunekawa, "Advanced LOS path loss model considered with the actual urban environment for microcellular mobile communications," *IEICE Technical Report*, RCS96-173, pp. 71-76, Feb. 1997 (in Japanese).
- [9] H. Masui, K. Takahashi, K. Kage, Y. Yamada, and S. Takahashi, "Difference of path-loss characteristics due to reception antenna heights in an urban LOS environment," in *IEEE Antennas Propagat. Soc. Int. Symp.*, Atlanta, GA, June 1998, pp. 1672-1675.